European Journal of Radiology 154 (2022) 110372

Contents lists available at ScienceDirect

European Journal of Radiology

journal homepage: www.elsevier.com/locate/ejrad

Evaluation of pathological complete response after neoadjuvant systemic treatment of invasive breast cancer using diffusion-weighted imaging compared with dynamic contrast-enhanced based kinetic analysis

Rie Ota [a,b,*], Masako Kataoka [a,*], Mami Iima [a,c], Maya Honda [a,d], Akane Ohashi [a,e], Ayami Ohno Kishimoto [a,f], Kanae Kawai Miyake [g], Yosuke Yamada [h], Yasuhide Takeuchi [h], Masakazu Toi [i], Yuji Nakamoto [a]

[a] Department of Diagnostic Imaging and Nuclear Medicine, Graduate School of Medicine Kyoto University, Kyoto, Japan
[b] Department of Radiology, Tenri Hospital, Nara, Japan
[c] Institute for Advancement of Clinical and Translational Science (iACT), Kyoto University Hospital, Kyoto, Japan
[d] Department of Diagnostic Radiology, Kansai Electric Power Hospital, Osaka, Japan
[e] Department of Diagnostic Radiology, National Hospital Organization Kyoto Medical Center, Kyoto, Japan
[f] Department of Diagnostic Radiology, Kyoto Katsura Hospital, Kyoto, Japan
[g] Department of Advanced Medical Imaging and Research, Graduate School of Medicine Kyoto University, Kyoto, Japan
[h] Department of Diagnostic Pathology, Kyoto University Hospital, Kyoto, Japan
[i] Department of Breast Surgery, Kyoto University Hospital, Kyoto, Japan

ARTICLE INFO

Keywords:
Neoadjuvant systemic treatment
Pathological complete response
Magnetic resonance imaging
Diffusion-weighted image
Kinetic assessment
Breast cancer

ABSTRACT

Purpose: This study compared the performance of diffusion-weighted imaging (DWI) to dynamic contrast-enhanced (DCE)-MRI for diagnosing pathological complete response (pCR) before surgery.

Method: Overall, 133 lesions from 133 patients who underwent pre-surgical MRI evaluation after neoadjuvant systemic treatment were included. Two readers blinded to the pathological diagnosis evaluated the images. MR images were obtained using a routine protocol sequence that included DWI and DCE-MRI. DWI of the target lesion was scored using a three-point scale. Kinetic patterns of lesions on DCE-MRI were scored using a four-point scale. The capacities of DWI and kinetic parameters for discriminating pCR and non-pCR were assessed via receiver operating characteristic (ROC) analysis.

Results: For DWI scores, ROC analysis showed areas under the ROC curve (AUCs) of 0.84 (95% confidence interval: 0.77–0.90) and 0.85 (0.77–0.90) for readers 1 and 2, respectively; corresponding AUCs of kinetic scores were 0.89 (0.82–0.94) and 0.88 (0.81–0.93). Among the triple-negative subtype, the AUCs of DWI scores were 0.84 (0.70–0.93) and 0.88 (0.75–0.96) for readers 1 and 2, respectively; corresponding AUCs of kinetic scores were 0.94 (0.83–0.99) and 0.93 (0.82–0.99). Among the luminal subtype, the AUCs of DWI scores were 0.85 (0.71–0.94) and 0.82 (0.68–0.92) for readers 1 and 2, respectively; corresponding AUCs of kinetic scores were 0.82 (0.68–0.92) and 0.72 (0.56–0.85).

Conclusions: Our DWI-based visual score and kinetic score showed similar diagnostic performances. Both DWI and kinetic scores tended to perform better in predicting pCR for the triple-negative subtype.

Abbreviations: NST, neoadjuvant systemic treatment; pCR, pathological complete response; DWI, diffusion-weighted imaging; DCE-MRI, dynamic contrast-enhanced magnetic resonance imaging; ADC, apparent diffusion coefficient; BI-RADS, Breast Imaging Report and Data System; ROC, receiver operating characteristic; CI, confidence interval; AUC, area under the ROC curve; ER, estrogen receptor; PgR, progesterone receptor; HER2, human epidermal growth factor receptor 2; RECIST, response evaluation criteria in solid tumors; CR, complete response; PR, partial response; SD, stable disease; PD, progressive disease.

* Corresponding authors.
E-mail addresses: ota_rie0624@kuhp.kyoto-u.ac.jp (R. Ota), makok@kuhp.kyoto-u.ac.jp (M. Kataoka).

https://doi.org/10.1016/j.ejrad.2022.110372
Received 14 September 2021; Received in revised form 21 April 2022; Accepted 23 May 2022
Available online 26 May 2022

1. Introduction

Neoadjuvant systemic treatment (NST), including chemotherapy and/or endocrine therapy, is commonly used for the treatment of breast cancer. NST facilitates downstaging of the primary breast tumor and avoidance of axillary lymph node metastasis [1]. Accurate evaluation of the response to NST provides important information concerning the impact of systemic therapies on breast cancer prognosis [2]. The achievement of a pathological complete response (pCR) after NST is important for surgery and outcome prediction. In multiple studies with large sample sizes, disease-free survival was better in the pCR group, particularly among patients with the triple-negative subtype [3 4 5 6]. Moreover, the tumor response to NST significantly impacts local regional therapy by reducing the tumor size, which facilitates breast-conserving surgery [7].

Dynamic contrast-enhanced magnetic resonance imaging (DCE-MRI) is the most accurate imaging modality for assessing the tumor response to NST, according to several studies [8 9 10]. However, multiple factors (e.g., cancer subtype and treatment regimen) can influence MRI accuracy [11]. Breast MRI tends to overestimate or underestimate the sizes of tumors that respond well to chemotherapy [12]. Currently, there is no evidence to support the possibility of avoiding surgery in cases of radiological complete response, but accurate prediction of pCR might increase the feasibility of minimizing surgery after NST [13 14].

A previous meta-analysis reported the accuracy of diffusion-weighted imaging (DWI) as a non-invasive and quantitative method to predict therapeutic response [15]. Some studies suggested that the accuracy of pCR diagnosis by MRI could be improved by using DWI along with conventional DCE-MRI [16 17]. This led to the hypothesis that the performance of DWI-based pre-surgical evaluation is equal to or better than DCE-MRI-based diagnosis. The use of DWI to visualize residual breast cancer might help to reduce the need for contrast agent. However, because of improvements in NST, residual tumors tend to be small, hindering a quantitative approach. Hence, there is a need for a scoring system based on visual assessment to ensure objectivity.

This study aimed to evaluate the use of DWI with a visually assessed scoring system for diagnosing pCR after NST, then compare the performance of DWI to the performance of DCE-MRI (including kinetic information).

2. Material and methods

2.1. Patients

Approval for this study protocol was obtained from the institutional review board of our hospital; the requirement for informed consent was waived because of the retrospective study design. The inclusion criteria were as follows: DCE-MRI performed after NST; receipt of NST; and pathological diagnosis performed at our hospital. Exclusion criteria were as follows: no MR images were obtained after NST; no receipt of NST; lack of post-contrast images; and poor image quality on DCE-MRI because of motion artifact. When both malignant and benign lesions were found in the ipsilateral breast, only the malignant lesion was used. When multiple malignant or multiple benign lesions were found in the ipsilateral breast, the lesion with the largest diameter in axial images was used. A flow chart summarizing the details of the patient selection process is shown in Supplementary Appendix A. In total, 133 women with 133 lesions (mean age, 50.0 years; age range, 26–74 years) who underwent pre-surgical MRI evaluation after NST from January 2014 to November 2020 were included in this study.

2.2. MRI protocol

MRI was performed using a Prisma/Trio Tim 3.0 Tesla scanner (Siemens AG, Erlangen, Germany) with 18- or 16-channel dedicated breast coils. MR images were obtained using a routine protocol sequence: T1-weighted image (T1WI), T2-weighted image (T2WI), DWI (b = 0, 1000 sec/mm^2), and DCE-MRI (pre-contrast and 1–2 min, and 5–6 min post-contrast). Details are summarized in Table 1.

2.3. Image interpretation and analysis

Images were evaluated using a workstation (Aquarius NET Viewer; TeraRecon, Foster City, CA, USA). Two board-certified radiologists specializing in breast imaging (reader 1 with 10 years of experience and reader 2 with 20 years of experience) independently evaluated the images. They were informed that all MR images had been acquired from patients with breast cancer, but they were blinded to the pathological diagnoses. For each reader, the reading sessions of DWI and DCE-MRI were scheduled with a 2-month interval. The readers evaluated DWI and DCE-MRI to identify residual lesions on post-NST images.

2.4. DWI score

After treatment, the readers were asked to identify residual lesions on DWI and apparent diffusion coefficient (ADC) maps alone; they were not allowed to refer to other images, such as T1WI, T2WI, or DCE-MRI. The readers were allowed to refer to pre-NST images (e.g., DWI and DCE-MRI) if the target lesion was not obvious on post-NST images. An ADC map was used for reference only. The readers were blinded to other imaging data (e.g., ultrasonography or mammography), clinical data, and pathological data.

DWI of the target lesion was evaluated and scored using a three-point scale: 2, obvious high signal intensity; 1, intermediate signal intensity in a scar-like shape; and 0, no abnormal signal intensity (Fig. 1). We applied the classification system used in the Breast Imaging Report and Data System (BI-RADS); we replaced contrast-enhanced areas on DCE-MRI with high signal intensity on DWI and classified the lesions as focus, mass, or non-mass. To determine whether the lesions identified by the two readers were identical, the morphology of the residual lesion (focus, mass, or non-mass) and its location were recorded by each reader.

ADC values were measured for all identifiable lesions by both readers. If a lesion was sufficiently large for region of interest (ROI) placement, the readers measured the values on ADC maps by placing a maximum of three ROIs of 3 mm in the lesion. ADC values were calculated only from lesions in which ROIs could be placed. In each ROI, the mean ADC values were calculated; the lowest of the mean ADC values

Table 1
MR imaging protocols.

Sequence	DWI SS-EPI	DCE-T1WI 3D-VIBE with fat suppression
Laterality	Bilateral	Bilateral
Orientation	Axial	Axial
TR/TE(ms)	Prisma:6300–6600/50, Trio:7600/62	3.7–3.8/1.4
FOV (mm^2)	330 × 160–187	330 × 330
Matrix	Prisma:162 × 92, Trio:166 × 80	384 × 346
Slice thickness (mm)	3.0	1.0
Slice number	48	144
b-Value (s/mm^2)	0, 1000	
Total acquisition time (min:s)	1:06	1:00
Parallel imaging acceleration factors	2	3
Time from contrast injection		early:60-120sec, delay:300-360sec

DWI, diffusion-weighted image; SS-EPI, single-shot echo-planar imaging; DCE-T1WI, dynamic contrast-enhanced T1WI; 3D-VIBE, 3D volumetric interpolated breath-hold examination; T1WI, T1-weighted image; T2WI, T2-weighted image; TR, repetition time; TE, echo time; FOV, field of view.

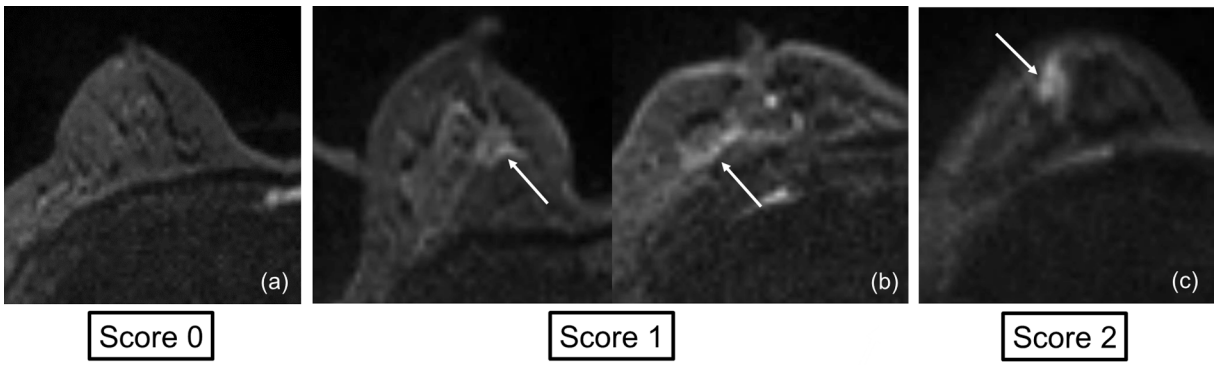

Fig. 1. DWI scores. DWI of the target lesion was evaluated and scored using a three-point scale. (a) Score 0: no abnormal signal intensity. (b) Score 1: intermediate signal intensity in a faint scar-like shape (arrows). (c) Score 2: obvious high signal intensity (arrow). No lesion sizes were included in the scoring method.

was used as the representative ADC value in each lesion. If a lesion size was insufficient for ROI placement, the readers measured the values on ADC maps by placing only one ROI of 3 mm in the lesion. Otherwise, the lesion was designated as "NA" (i.e., difficult to measure).

2.5. Kinetic score

After treatment completion, the readers were asked to identify residual lesions on DCE-MRI. To identify the target lesion, the readers could refer to pre-NST MRI findings, including DCE-MRI and DWI. The readers were blinded to other imaging information, as noted above in the DWI score section.

The kinetic score of each identified lesion was based on kinetic curve analysis by placing one ROI of 3 mm in diameter in the most intensely enhanced area.

In accordance with the definition used by the BI-RADS 5th edition, the signal intensity (SI) increase was defined as (SI delay − SI early)/SI pre × 100% and divided into three categories: persistent, > 10% of the SI increase; plateau, ≥−10% and ≤10% of the SI increase; and washout, < −10% of the SI increase. The kinetic score was allocated based on the enhancement pattern on delayed phase as follows: 0, no enhancement; 1, persistent; 2, plateau; and 3, washout. Lesions with insufficient size for ROI placement were classified as "difficult to measure.".

2.6. Pathological evaluation

Histopathological information regarding the biopsied or surgical specimens was extracted from pathology reports that had been generated at the time of treatment. The diagnoses were made by one of four board-certified pathologists with at least 16 years of experience. The presence of residual lesions was considered a positive result. pCR was histopathologically defined as the absence of residual invasive cancer in surgically resected breast tissue. Residual in situ lesions without invasion were included in pCR. On the basis of their immunohistochemical profiles, breast cancers were divided into four immunohistochemical subtypes. The triple-negative subtype was represented by negativity for estrogen receptor (ER), progesterone receptor (PgR), and human epidermal growth factor 2 (HER2). The luminal subtype was defined as ER- or PgR-positive and HER2-negative.

2.7. Statistical analysis

Statistical analysis was performed using MedCalc Statistical Software version 19.2.1 (MedCalc Software Ltd., Ostend, Belgium). The inter-rater reliabilities of the DWI and kinetic scores between the two readers were calculated using Cohen's weighted kappa coefficient [18]. The diagnostic performances of DWI parameters in identifying residual invasive component (non-pCR) were assessed using receiver operating characteristic (ROC) analysis. DeLong et al. presented a nonparametric approach to the analysis of areas under correlated ROC curves, using generalized U-statistics theory to generate an estimated covariance matrix [19]. The threshold values determined using the method of DeLong et al. were used to calculate the sensitivity and specificity of identifying the residual invasive component.

Inter-method variabilities were assessed by weighted kappa coefficients for categorical data. A kappa value of 0.01–0.20 represented poor agreement, while 0.21–0.40 was considered fair, 0.41–0.60 was considered moderate, 0.61–0.80 was considered good, and 0.81–1.00 was considered very good [20].

3. Results

3.1. Lesion characteristics

In accordance with pre-determined inclusion/exclusion criteria (see Supplementary Appendix A), 133 patients were selected. Among them, 43.6% (58/133) of cases achieved pCR, while 56.4% (75/133) were categorized as non-pCR according to postoperative pathology evaluation. The mean time between the preoperative DCE-MRI and surgery was 17.5 days. The lesion characteristics are described in Table 2. The mean pre-treatment tumor diameters in DCE-MRI were 31.2 mm (range, 9–89 mm) for reader 1 and 33.2 mm (range, 9–90 mm) for reader 2. For 117 mass lesions, the mean pre-treatment tumor diameters in DCE-MRI were 30.4 (range, 11–89 mm) for reader 1 and 32.2 mm (range, 12–90 mm) for reader 2. For 16 non-mass lesions, the mean pre-treatment tumor diameters in DCE-MRI were 37.3 mm (range, 9–78 mm) for reader 1 and 40.8 mm (range, 9–90 mm) for reader 2.

3.2. DWI score

The distribution of DWI scores is shown in Table 3. The size

Table 2
Summary of lesion characteristics.

Classification		n = 133 (%)
Histology	IC	119 (89.5%)
	ILC	2 (1.5%)
	IMPC	6 (4.5%)
	MC	2 (1.5%)
	Other	4 (3.0%)
Subtype	ER and PgR–/HER2– (Triple-negative)	45 (33.8%)
	ER or PgR+/HER2– (Luminal)	43 (32.3%)
	ER and PgR–/HER2+ (HER2-positive)	18 (13.5%)
	ER or PgR+/HER2+ (Luminal/HER2)	27 (20.3%)

IC, invasive carcinoma of no special type; ILC, invasive lobular carcinoma; IMPC, invasive micropapillary carcinoma; MC, mucinous carcinoma; other (including two metaplastic carcinomas and one invasive apocrine carcinoma); ER, estrogen receptor; PgR, progesterone receptor; HER2, human epidermal growth factor 2.

Table 3
DWI scores of lesions according to breast cancer subtype.

n = 133		pCR				Non-pCR				Total			
DWI score		0	1	2	Total	0	1	2	Total	0	1	2	Total
Reader 1	Triple-negative	16	6	3	25	2	4	14	20	18	10	17	45
	Luminal	3	2	1	6	2	4	31	37	5	6	32	43
	HER2-positive	6	5	2	13	0	2	3	5	6	7	5	18
	Luminal/HER2	9	2	3	14	2	1	10	13	11	3	13	27
	Total	34	15	9	58	6	11	58	75	40	26	67	133
Reader 2	Triple-negative	15	7	3	25	2	4	14	20	17	11	17	45
	Luminal	3	2	1	6	3	6	28	37	6	8	29	43
	HER2-positive	5	7	1	13	0	2	3	5	5	9	4	18
	Luminal/HER2	9	3	2	14	2	3	8	13	11	6	10	27
	Total	32	19	7	58	7	15	53	75	39	34	60	133

distribution of non-pCR lesions for the DWI score is shown in Supplementary Appendix B. The DWI scores of the two readers were in agreement for 119 lesions (89.5%), with a kappa value of 0.87 (95% confidence interval [CI]: 0.80–0.94), suggesting very good agreement.

ROC analysis showed areas under the ROC curve (AUCs) of 0.84 (95% CI: 0.77–0.90) for reader 1 and 0.85 (95% CI: 0.77–0.90) for reader 2 (Figs. 2 and 3).

Cases with a DWI score of 0 were pCR except for six false-negative lesions for reader 1 and seven false-negative lesions for reader 2. False-negative cases for the DWI score included two invasive lobular carcinomas (ILCs), one invasive micropapillary carcinoma, and other invasive carcinomas of no special type for readers 1 and 2.

ADC values of the lesions were also measured by placing 3-mm circular ROIs. However, ADC values could not be measured because of small lesion sizes and scar-like shapes in 46/135 cases for reader 1 and in 42/135 cases for reader 2. Further analyses of ADC values were not performed because of these missing data.

3.3. Kinetic score

The distribution of kinetic scores is shown in Table 4. The kinetic scores of the two readers were in agreement for 110 lesions (66.3%), with a kappa value of 0.84 (95% CI: 0.77–0.91), suggesting very good agreement.

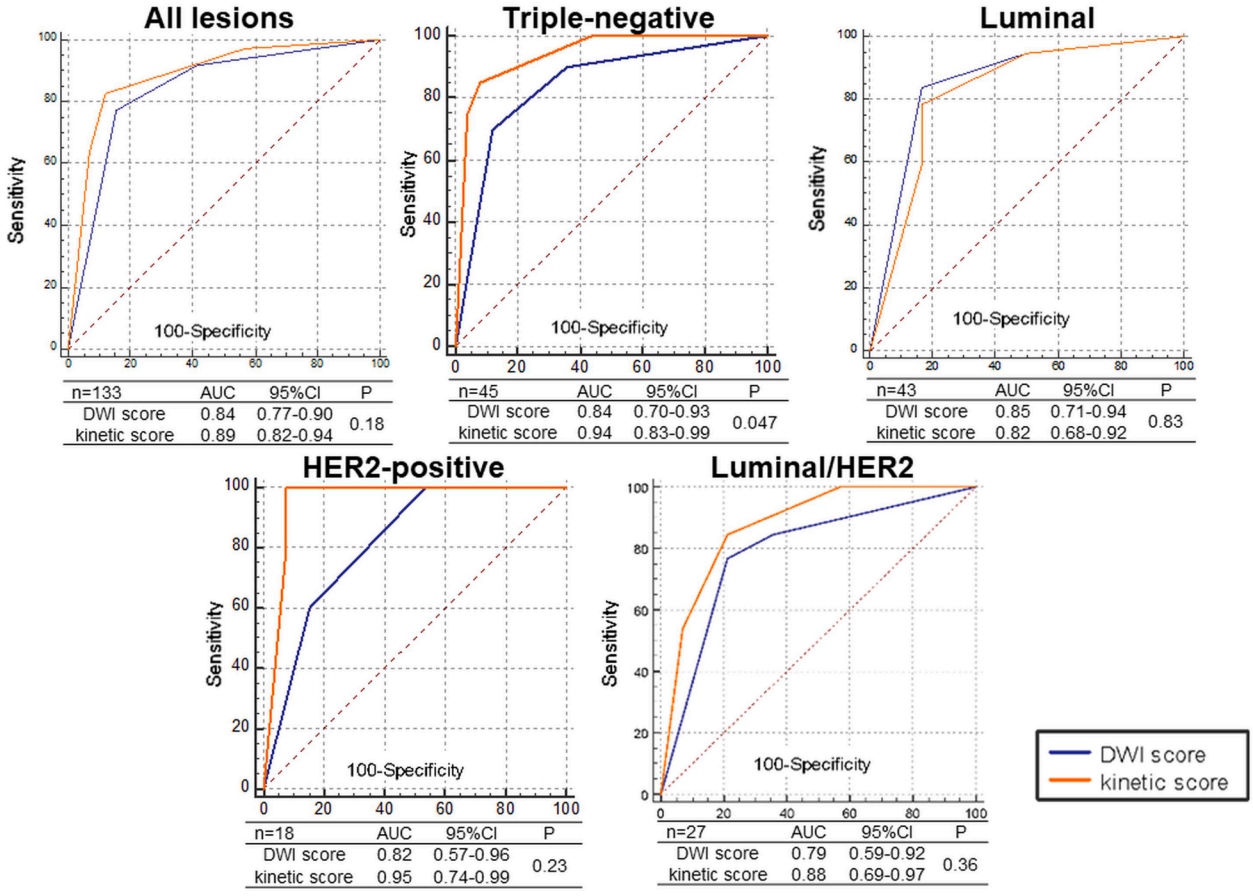

Fig. 2. Pairwise comparison of ROC analysis for diagnosing pCR according to the DWI and kinetic scores (reader 1). Using the DeLong method with Bonferroni correction, a pairwise comparison of ROC curves was performed. There were no significant differences in AUCs between the DWI score and the kinetic score (p = 0.18). The kinetic score showed a slightly higher AUC, while its 95% confidence interval overlapped with the 95% confidence interval of the DWI score. Both the kinetic score and the DWI score demonstrated excellent diagnostic performance for the triple-negative subtype compared with the other subtypes, with AUCs of 0.84–0.94.

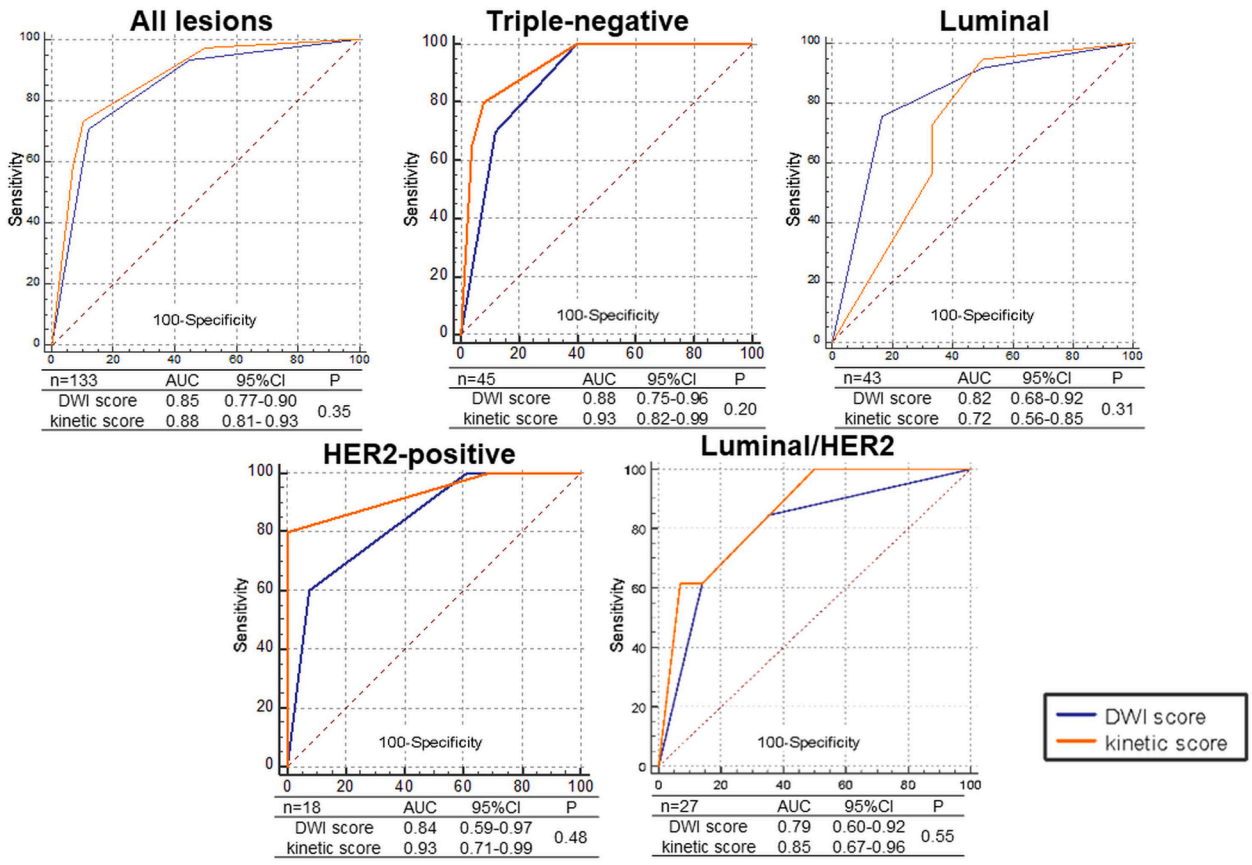

Fig. 3. Pairwise comparison of ROC analysis for diagnosing pCR according to the DWI and kinetic scores (reader 2). Using the DeLong method with Bonferroni correction, a pairwise comparison of ROC curves was performed. There were no significant differences in AUCs between the DWI score and the kinetic score ($p = 0.35$). The kinetic score showed a slightly higher AUC, while its 95% confidence interval overlapped with the 95% confidence interval of the DWI score. Both the kinetic score and the DWI score demonstrated excellent diagnostic performance for the triple-negative subtype compared with the other subtypes, with AUCs of 0.88–0.93. For the luminal subtype, the DWI score tended to perform better than the kinetic score.

Table 4
Kinetic scores of lesions according to breast cancer subtype.

n = 133		pCR					Non-pCR					Total				
kinetic score		0	1	2	3	Total	0	1	2	3	Total	0	1	2	3	Total
Reader 1	Triple-negative	14	9	1	1	25	0	3	2	15	20	14	12	3	16	45
	Luminal	3	2	0	1	6	2	6	7	22	37	5	8	7	23	43
	HER2-positive	2	10	0	1	13	0	0	1	4	5	2	10	1	5	18
	Luminal/HER2	6	5	2	1	14	0	2	4	7	13	6	7	6	8	27
	Total	25	26	3	4	58	2	11	14	48	75	27	37	17	52	133
Reader 2	Triple-negative	15	8	1	1	25	0	4	3	13	20	15	12	4	14	45
	Luminal	3	1	0	2	6	2	8	6	21	37	5	9	6	23	43
	HER2-positive	4	9	0	0	13	0	1	2	2	5	4	10	2	2	18
	Luminal/HER2	7	5	1	1	14	0	5	0	8	13	7	10	1	9	27
	Total	29	23	2	4	58	2	18	11	44	75	31	41	13	48	133

ROC analysis showed AUCs of 0.89 (95% CI: 0.82–0.94) for reader 1 and 0.88 (95% CI: 0.81–0.93) for reader 2 (Figs. 2 and 3).

Cases with a kinetic score of 0 were pCR except for two false-negative lesions: one ILC (also included in the false-negative cases for the DWI score) and one invasive carcinoma of no special type.

Using the DeLong method with Bonferroni correction, pairwise comparison of ROC curves was performed [19]. There were no significant differences in the AUCs of the DWI scores and the kinetic scores for reader 1 ($p = 0.18$) and reader 2 ($p = 0.35$).

The sensitivity and specificity of the DWI/kinetic scores are summarized in Table 5.

3.4. Sub-analysis by subtype

3.4.1. Triple-negative subtype

Among 45 lesions of the triple-negative subtype, 55.6% (25/45) of cases achieved pCR. The distribution of DWI scores is shown in Table 3. ROC analysis of DWI scores showed AUCs of 0.84 (95% CI: 0.70–0.93) for reader 1 and 0.88 (95% CI: 0.75–0.96) for reader 2 (Figs. 2 and 3).

The distribution of kinetic scores is shown in Table 4. ROC analysis of kinetic scores showed AUCs of 0.94 (95% CI: 0.83–0.99) for reader 1 and 0.93 (95% CI: 0.82–0.99) for reader 2 (Figs. 2 and 3).

There were borderline significant differences in AUCs between DWI scores and kinetic scores for reader 1 ($p = 0.047$), while there were no significant differences in AUCs between DWI scores and kinetic scores

Table 5
Diagnostic performance of DWI scores/kinetic scores in the diagnosis of pCR in breast cancer subtypes by two readers.

	All lesions (n = 133)		TN subtype (n = 45)		Luminal subtype (n = 43)		HER2-positive subtype (n = 18)		Luminal/HER2 subtype (n = 27)	
Criterion	Sensitivity (%)	Specificity (%)	Sensitivity (%)	Specificity (%)	Sensitivity (%)	Specificity (%)	Sensitivity (%)	Specificity (%)	Sensitivity (%)	Specificity (%)
DWI score										
Reader 1										
> 0	92.0	58.6	90.0	64.0	94.6	50.0	100.0	46.2	84.6	64.3
> 1	77.3	84.5	70.0	88.0	83.8	83.3	60.0	84.6	76.9	78.6
Reader 2										
> 0	93.3	55.2	100.0	60.0	91.9	50.0	100.0	38.5	84.6	64.3
> 1	70.7	87.9	70.0	88.0	75.7	83.3	60.0	92.3	61.5	85.7
Kinetic score										
Reader 1										
> 0	97.3	43.1	100.0	56.0	94.6	50.0	100.0	15.4	100.0	42.9
> 1	82.7	87.9	85.0	92.0	78.4	83.3	100.0	92.3	84.6	78.6
> 2	64.0	93.1	75.0	96.0	59.5	83.3	80.0	92.3	53.9	92.9
Reader 2										
> 0	97.3	50.0	100.0	60.0	94.6	50.0	100.0	30.8	100.0	50.0
> 1	73.3	89.7	80.0	92.0	73.0	66.7	80.0	100.0	61.5	85.7
> 2	58.7	93.1	65.0	96.0	56.8	66.7	40.0	100.0	61.5	92.9

Score > 0: score 0 was classified as pCR; scores 1, 2 and 3 were classified as non-pCR.
Score > 1: scores 0 and 1 were classified as pCR; scores 2 and 3 were classified as non-pCR.
Score > 2: scores 0, 1 and 2 were classified as pCR; scores 3 were classified as non-pCR.

for reader 2 (p = 0.20). We present one case of triple-negative cancer in Fig. 4.

3.4.2. *Luminal subtype*

Among 43 lesions of the luminal subtype defined as hormone receptor-positive and HER2-negative, 14.0% (6/43) of cases achieved pCR. The distribution of DWI scores is shown in Table 3. ROC analysis showed AUCs of 0.85 (95% CI: 0.71–0.94) for reader 1 and 0.82 (95% CI: 0.68–0.92) for reader 2 (Figs. 2 and 3).

The distribution of kinetic scores is shown in Table 4. ROC analysis showed AUCs of 0.82 (95% CI: 0.68–0.92) for reader 1 and 0.72 (95% CI: 0.56–0.85) for reader 2 (Figs. 2 and 3). Although there were no significant differences in AUCs between DWI scores and kinetic scores for reader 1 (p = 0.83) and reader 2 (p = 0.31), the AUCs for both readers tended to be better when using DWI scores than when using kinetic scores.

3.4.3. *HER2-positive subtype*

Among 18 lesions of the HER2-positive subtype, 72.2% (13/18) of cases achieved pCR.

The distribution of DWI scores is shown in Table 3. ROC analysis showed AUCs of 0.82 (95% CI: 0.57–0.96) for reader 1 and 0.84 (95% CI: 0.59–0.97) for reader 2 (Figs. 2 and 3). The distribution of kinetic scores is shown in Table 4. ROC analysis showed AUCs of 0.95 (95% CI: 0.82–0.93) for reader 1 and 0.93 (95% CI: 0.71–0.99) for reader 2 (Figs. 2 and 3). There were no significant differences in AUCs between DWI scores and kinetic scores for reader 1 (p = 0.23) and reader 2 (p = 0.48).

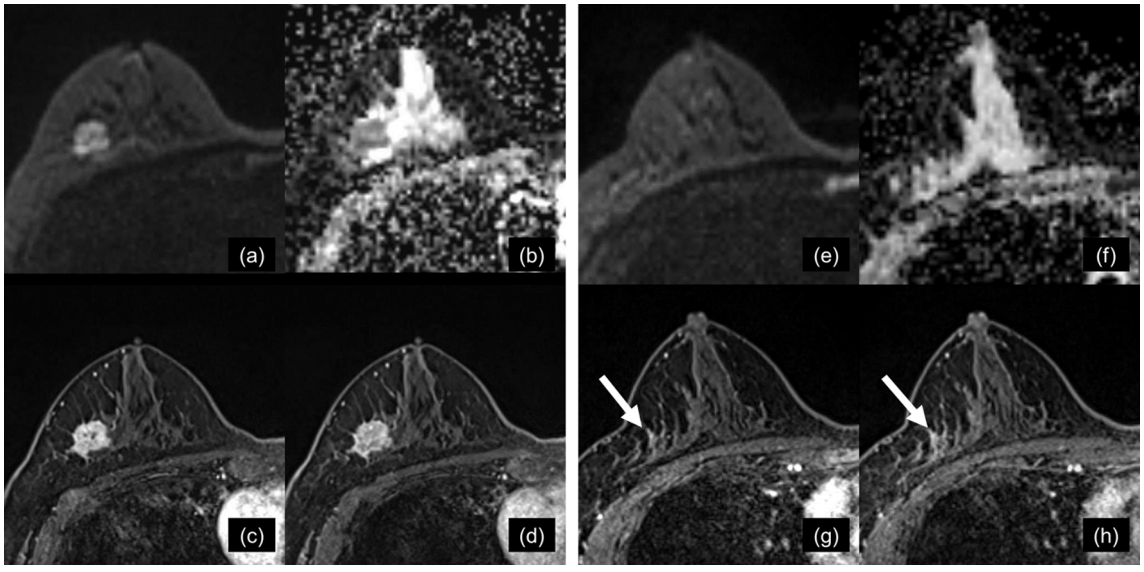

Fig. 4. (a) Pre-NST DWI. (b) Pre-NST ADC map. (c) Pre-NST DCE-MRI early phase. (d) Pre-NST DCE-MRI delay phase. (e) Post-NST DWI. (f) Post-NST ADC map. (g) Post-NST DCE-MRI early phase. (h) Post-NST DCE-MRI delay phase. Right triple-negative breast cancer in a 64-year-old patient who underwent NST for invasive carcinoma. Pre-NST MRI showed a 22-mm mass on DWI and DCE-MRI. After treatment, no high signal intensity remained on DWI; focal enhancement with persistent kinetics was observed on DCE-MRI (g, h, arrow). The DWI score was 0 and the kinetic score was 1. The patient underwent surgery and had no residual disease. Both the DWI score and the kinetic score suggested a correct diagnosis.

3.4.4. Luminal/HER2 subtype

Hormone receptor-positive and HER2-positive tumors were regarded as luminal/HER2 tumors in this analysis. Among 27 lesions of the luminal/HER2 subtype, 51.9% (14/27) of cases achieved pCR.

The distribution of DWI scores is shown in Table 3. ROC analysis showed AUCs of 0.79 (95% CI: 0.59–0.92) for reader 1 and 0.79 (95% CI: 0.60–0.92) for reader 2 (Figs. 2 and 3). The distribution of kinetic scores is shown in Table 4. ROC analysis showed AUCs of 0.88 (95% CI: 0.69–0.97) for reader 1 and 0.85 (95% CI: 0.67–0.96) for reader 2 (Figs. 2 and 3). There were no significant differences in AUCs between DWI scores and kinetic scores for reader 1 ($p = 0.36$) and reader 2 ($p = 0.55$).

3.5. RECIST-based evaluation

Response is typically measured using the response evaluation criteria in solid tumors (RECIST). Complete response (CR) is defined as complete disappearance of the tumor, near CR is defined as near disappearance with equivocal weak enhancement, partial response (PR) is defined as a decrease in the sum of the longest axes of all individual lesions by ≥30%, progressive disease (PD) is defined as an increase in this sum by ≥20%, and the remaining clinical manifestations are classified as stable disease (SD). RECIST-based evaluation is categorized using a three-point scale: 2, PD/SD/PR; 1, near CR; and 0, CR.

We performed pairwise comparisons of ROC curves between RECIST scores and DWI/kinetic scores. There were no significant differences in AUCs between DWI scores and RECIST scores ($p = 0.58$) or between kinetic scores and RECIST scores ($p = 0.30$) for reader 1. The AUC of RECIST scores was higher than the AUC of DWI scores, but lower than the AUC of kinetic scores.

There were also no significant differences in AUCs between DWI scores and RECIST scores ($p = 0.67$) or between kinetic scores and RECIST scores ($p = 0.09$) for reader 2. The AUC of RECIST scores was lower than the AUCs of DWI and kinetic scores (see Supplementary Appendix C).

4. Discussion

Our results suggest that the DWI-based visual analysis and kinetic analysis showed similar diagnostic performances. The kinetic analysis may examine vascularity as a marker of viable residual tumor, while DWI-based images are associated with the cellular component of residual tumor. To our knowledge, the current study is unique in its use of visual assessments of DWI for residual tumor; this method is easily applied in clinical practice and is feasible for small lesions.

Numerous studies have used DWI in the evaluation of pCR [15,21 22 23 24,2526]. For example, the diagnostic performance of the generally high sensitivity and high specificity of DWI for diagnosing pCR in patients with breast cancer was reviewed in a meta-analysis [15]. Gao et al. evaluated the accuracy of DWI in the detection of pCR to NACT in patients with breast cancer. Twenty studies with 1490 total participants were enrolled in their analysis. Their pooled estimates revealed a sensitivity of 0.89 (95% CI: 0.86–0.91) and a specificity of 0.72 (95% CI: 0.68–0.75). ADC values have frequently been used for quantitative assessment of DWI. The American College of Radiology Imaging Network (ACRIN) 6698 performed a sub-study of the Investigation of Serial Studies to Predict Your Therapeutic Response with Imaging and Molecular analysis 2 (I-SPY 2) trial to identify more effective breast cancer treatments [21]. The results demonstrated that changes in tumor ADC after 12 weeks of therapy alone were predictive of pCR. Considering that most studies regarding DWI for the assessment of treatment response have been conducted at single centers [22 23 24], ACRIN 6698 findings are important for validating ADC as a biomarker for predicting pCR. Recently, texture analysis and machine learning have been applied to DWI and DCE-MRI data to improve the prediction performance of pCR [22 23]. Zhang et al. reported that the optimal methods for measuring ADC values may vary among shrinkage patterns in luminal tumors [24].

Several studies demonstrated that changes in the ADC measured from DWI of pre-treatment and post-treatment MRI were predictive of pCR in patients with breast cancer who received neoadjuvant chemotherapy [27 28]. Another study demonstrated that changes in the ADC after chemotherapy were more closely correlated with pathological outcome and prognosis than were changes in tumor size [29]. However, evaluations based on ADC values require a sufficiently large lesion size for reliable measurement; thus, such evaluations are difficult to conduct for small lesions after NST. Additionally, the neoadjuvant chemotherapy effect is recognized as a fibrous or fibromyxoid area; lesions with low water content may exhibit a very low signal at both $b = 0$ s/mm^2 and $b = 800$ s/mm^2, resulting in poor images and artificially low ADC values because of signal-blackout in such lesions [30]. These low ADC values are not indicative of true diffusion restriction; evaluation of these lesions using ADC alone might lead to erroneous interpretation of breast DWI. These problems can be avoided by using our DWI scoring system that is based on signal intensity. Importantly, the ADC values could not be measured in >30% of cases for both readers in the present study. Therefore, visual assessments (e.g., DWI score) may be practical. Considering the single-center retrospective design of this study, validations in larger multi-center cohorts (such as the ACRIN 6698 [21,25]) are needed.

Residual tumor size and kinetics assessments have been used for objective measurements of residual disease and treatment response [31]. Compared with clinical assessments, MRI findings are a stronger predictor of pathological response to NST; their greatest advantage lies in the volumetric measurement of tumor response during early treatment [32]. Evaluations of RECIST-based and other size-based methods are easy to implement, but their performances remain inferior to kinetics-based evaluation [33]. Functional tumor volume (FTV) assessment uses MRI to determine both tumor volume and kinetics; this assessment method can predict recurrence-free survival in patients who receive neoadjuvant chemotherapy for breast cancer [34]. The suitability of quantifying kinetic heterogeneity derived from breast DCE-MRI for the prediction of neoadjuvant treatment response has been assessed through pre-treatment imaging examinations [33]. These kinetic-based methods perform better than conventional size-based methods; they may be ideal for residual tumor prediction and measurement. However, the findings are retrospectively analyzed using dedicated software, which hinders broader use of these methods in clinical practice. Additionally, this quantitative analysis might be inaccurate for small and weakly enhanced residual lesions. Because the DWI and kinetic scores are based on visual evaluations, our method is easy to implement in clinical practice. Visual evaluation-based scoring is often feasible, even for lesions that are small and difficult to measure.

An important finding in the current study was that the accuracy of MRI in estimating post-NST prediction of pCR varied according to subtype. Both the kinetic and DWI scores performed better for the triple-negative subtype than for the other subtypes in predicting pCR, with AUCs of nearly 90%. These findings could be attributed to the good response rate of triple-negative breast cancer to chemotherapy. For the luminal subtype, estimations of residual tumor tended to be less accurate; the AUC of the DWI score tended to be better than the AUC of the kinetic score. The above results indicate the need for subtype-specific strategies when evaluating residual tumor after NST.

Subtype-specific response evaluation by DCE-MRI or DWI has recently been explored. Several investigations involving DCE-MRI showed that the accuracy of MRI in predicting pCR was highest for the triple-negative subtype and lowest for the luminal subtype [35], consistent with our findings. Our study population was enriched in the triple-negative subtype (34%), partly because neoadjuvant chemotherapy is proposed for the triple-negative subtype more often than for other subtypes.

Some false-negative cases were identified when assessing the presence of residual tumor based on the DWI and kinetic scores. For two

ILCs, it was difficult to evaluate residual tumors using both kinetic and DWI scores. Non-mass-like ILCs may contain interspersed normal fibroglandular tissue or fat tissue, which can affect the evaluation of pCR. The other case involved an invasive carcinoma with the luminal subtype. In contrast, there were no false-negative cases among lesions with the triple-negative subtype.

Our study had several limitations. First, it used a retrospective design. Second, because we did not compare the lesion sizes on images with the pathological findings, we could not stratify the pathological characteristics according to lesion size. Third, this study depended on the readers' subjective visual assessments. Fourth, we defined pCR as the absence of invasive cancer, with or without the presence of ductal carcinoma in situ. Fifth, the per-subtype analysis was exploratory because of the small sample size, particularly for HER2-positive tumors (n = 18). Sixth, there were borderline significant differences in AUCs between the DWI scores and kinetic scores for reader 1. This finding may be related to the small sample size; the difference should be verified in a larger cohort. Finally, the combined effect of the DWI and kinetic scores was not examined. Superior results could be obtained by adding DWI to the kinetic evaluation; this approach will be explored in subsequent research.

In conclusion, the DWI score showed excellent performance in estimating residual tumor after NST; its diagnostic performance was similar to the diagnostic performance of the kinetic score. These results imply the potential of applying DWI to the evaluation of breast MRI after NST. In particular, triple-negative breast cancers with low DWI and kinetic scores are associated with pCR.

Declaration of Competing Interest

The authors declare that they have no known competing financial interests or personal relationships that could have appeared to influence the work reported in this paper.

Acknowledgments

We thank Yuta Urushibata for his technical support. We also thank H. Nikki March, PhD, and Ryan Chastain-Gross, Ph.D., from Edanz (https://jp.edanz.com/ac) for editing a draft of this manuscript.

Appendix A. Supplementary material

Supplementary data to this article can be found online at https://doi.org/10.1016/j.ejrad.2022.110372.

References

[1] J.R. Gralow, H.J. Burstein, W. Wood, G.N. Hortobagyi, L. Gianni, G. von Minckwitz, A.U. Buzdar, I.E. Smith, W.F. Symmans, B. Singh, E.P. Winer, Preoperative therapy in invasive breast cancer: pathologic assessment and systemic therapy issues in operable disease, J. Clin. Oncol. 26 (2008) 814–819.

[2] G. von Minckwitz, J.U. Blohmer, S.D. Costa, C. Denkert, H. Eidtmann, W. Eiermann, B. Gerber, C. Hanusch, J. Hilfrich, J. Huober, C. Jackisch, M. Kaufmann, S. Kummel, S. Paepke, A. Schneeweiss, M. Untch, D.M. Zahm, K. Mehta, S. Loibl, Response-guided neoadjuvant chemotherapy for breast cancer, J. Clin. Oncol. 31 (2013) 3623–3630.

[3] P. Rastogi, S.J. Anderson, H.D. Bear, C.E. Geyer, M.S. Kahlenberg, A. Robidoux, R. G. Margolese, J.L. Hoehn, V.G. Vogel, S.R. Dakhil, D. Tamkus, K.M. King, E. R. Pajon, M.J. Wright, J. Robert, S. Paik, E.P. Mamounas, N. Wolmark, Preoperative chemotherapy: updates of National Surgical Adjuvant Breast and Bowel Project Protocols B-18 and B-27, J. Clin. Oncol. 26 (2008) 778–785.

[4] G. von Minckwitz, M. Untch, J.U. Blohmer, S.D. Costa, H. Eidtmann, P.A. Fasching, B. Gerber, W. Eiermann, J. Hilfrich, J. Huober, C. Jackisch, M. Kaufmann, G. E. Konecny, C. Denkert, V. Nekljudova, K. Mehta, S. Loibl, Definition and impact of pathologic complete response on prognosis after neoadjuvant chemotherapy in various intrinsic breast cancer subtypes, J. Clin. Oncol. 30 (2012) 1796–1804.

[5] K.R. Broglio, M. Quintana, M. Foster, M. Olinger, A. McGlothlin, S.M. Berry, J.-F. Boileau, C. Brezden-Masley, S. Chia, S. Dent, K. Gelmon, A. Paterson, D. Rayson, D.A. Berry, Association of Pathologic Complete Response to Neoadjuvant Therapy in HER2-Positive Breast Cancer With Long-Term Outcomes: A Meta-Analysis, JAMA Oncol 2 (6) (2016) 751, https://doi.org/10.1001/jamaoncol.2015.6113.

[6] P. Cortazar, L. Zhang, M. Untch, K. Mehta, J.P. Costantino, N. Wolmark, H. Bonnefoi, D. Cameron, L. Gianni, P. Valagussa, S.M. Swain, T. Prowell, S. Loibl, D.L. Wickerham, J. Bogaerts, J. Baselga, C. Perou, G. Blumenthal, J. Blohmer, E. P. Mamounas, J. Bergh, V. Semiglazov, R. Justice, H. Eidtmann, S. Paik, M. Piccart, R. Sridhara, P.A. Fasching, L. Slaets, S. Tang, B. Gerber, C.E. Geyer, R. Pazdur, N. Ditsch, P. Rastogi, W. Eiermann, G. von Minckwitz, Pathological complete response and long-term clinical benefit in breast cancer: the CTNeoBC pooled analysis, Lancet 384 (9938) (2014) 164–172.

[7] H.M. Kuerer, M. Vrancken Peeters, D.W. Rea, M. Basik, J. De Los Santos, J. Heil, Nonoperative Management for Invasive Breast Cancer After Neoadjuvant Systemic Therapy: Conceptual Basis and Fundamental International Feasibility Clinical Trials, Ann. Surg. Oncol. 24 (2017) 2855–2862.

[8] Q. Cheng, J. Huang, J. Liang, M. Ma, K. Ye, C. Shi, L. Luo, The Diagnostic Performance of DCE-MRI in Evaluating the Pathological Response to Neoadjuvant Chemotherapy in Breast Cancer: A Meta-Analysis, Front. Oncol. 10 (2020) 93.

[9] G. Mariscotti, N. Houssami, M. Durando, L. Bergamasco, P.P. Campanino, C. Ruggieri, E. Regini, A. Luparia, R. Bussone, A. Sapino, P. Fonio, G. Gandini, Accuracy of mammography, digital breast tomosynthesis, ultrasound and MR imaging in preoperative assessment of breast cancer, Anticancer Res. 34 (2014) 1219–1225.

[10] Y. Tokuda, M. Yanagawa, Y. Fujita, K. Honma, T. Tanei, M. Shimoda, T. Miyake, Y. Naoi, S.J. Kim, K. Shimazu, S. Hamada, N. Tomiyama, Prediction of pathological complete response after neoadjuvant chemotherapy in breast cancer: comparison of diagnostic performances of dedicated breast PET, whole-body PET, and dynamic contrast-enhanced MRI, Breast Cancer Res. Treat. 188 (2021) 107–115.

[11] M.L. Marinovich, N. Houssami, P. Macaskill, F. Sardanelli, L. Irwig, E. P. Mamounas, G. von Minckwitz, M.E. Brennan, S. Ciatto, Meta-analysis of magnetic resonance imaging in detecting residual breast cancer after neoadjuvant therapy, J. Natl Cancer Inst. 105 (2013) 321–333.

[12] E.L. Rosen, K.L. Blackwell, J.A. Baker, M.S. Soo, R.C. Bentley, D. Yu, T.V. Samulski, M.W. Dewhirst, Accuracy of MRI in the detection of residual breast cancer after neoadjuvant chemotherapy, AJR Am. J. Roentgenol. 181 (2003) 1275–1282.

[13] A. Morvan, B. de Korvin, C. Bouriel, A. Carsin, P. Tas, C. Bendavid, P.F. Dupré, P. Kerbrat, H. Mesbah, P. Poree, J. Levêque, MRI evaluation of residual breast carcinoma after neoadjuvant chemotherapy, J. Radiol. 91 (2010) 693–699.

[14] M.B.I. Lobbes, R. Prevos, M. Smidt, V.C.G. Tjan-Heijnen, M. van Goethem, R. Schipper, R.G. Beets-Tan, J.E. Wildberger, The role of magnetic resonance imaging in assessing residual disease and pathologic complete response in breast cancer patients receiving neoadjuvant chemotherapy: a systematic review, Insights, Imaging 4 (2) (2013) 163–175.

[15] W. Gao, N. Guo, T. Dong, Diffusion-weighted imaging in monitoring the pathological response to neoadjuvant chemotherapy in patients with breast cancer: a meta-analysis, World J Surg Oncol 16 (2018) 145.

[16] G. Santamaría, X. Bargalló, P.L. Fernández, B. Farrús, X. Caparrós, M. Velasco, Neoadjuvant Systemic Therapy in Breast Cancer: Association of Contrast-enhanced MR Imaging Findings, Diffusion-weighted Imaging Findings, and Tumor Subtype with Tumor Response, Radiology 283 (2017) 663–672.

[17] R. Woodhams, S. Kakita, H. Hata, K. Iwabuchi, M. Kuranami, S. Gautam, H. Hatabu, S. Kan, C. Mountford, Identification of residual breast carcinoma following neoadjuvant chemotherapy: diffusion-weighted imaging–comparison with contrast-enhanced MR imaging and pathologic findings, Radiology 254 (2010) 357–366.

[18] J. Cohen, A coefficient of agreement for nominal scales, Educ. Measur. Psychol. 20 (1) (1960) 37–46.

[19] E.R. DeLong, D.M. DeLong, D.L. Clarke-Pearson, Comparing the areas under two or more correlated receiver operating characteristic curves: a nonparametric approach, Biometrics 44 (1988) 837–845.

[20] J.R. Landis, G.G. Koch, The measurement of observer agreement for categorical data, Biometrics 33 (1977) 159–174.

[21] S.C. Partridge, Z. Zhang, D.C. Newitt, J.E. Gibbs, T.L. Chenevert, M.A. Rosen, P. J. Bolan, H.S. Marques, J. Romanoff, L. Cimino, B.N. Joe, H.R. Umphrey, H. Ojeda-Fournier, B. Dogan, K. Oh, H. Abe, J.S. Drukteinis, L.J. Esserman, N.M. Hylton, A.T. Team, I.S.T. Investigators, Diffusion-weighted MRI Findings Predict Pathologic Response in Neoadjuvant Treatment of Breast Cancer: The ACRIN 6698 Multicenter Trial, Radiology 289 (2018) 618–627.

[22] A. Tahmassebi, G.J. Wengert, T.H. Helbich, Z. Bago-Horvath, S. Alaei, R. Bartsch, P. Dubsky, P. Baltzer, P. Clauser, P. Kapetas, E.A. Morris, A. Meyer-Baese, K. Pinker, Impact of Machine Learning With Multiparametric Magnetic Resonance Imaging of the Breast for Early Prediction of Response to Neoadjuvant Chemotherapy and Survival Outcomes in Breast Cancer Patients, Invest. Radiol. 54 (2019) 110–117.

[23] N.L. Eun, D. Kang, E.J. Son, J.S. Park, J.H. Youk, J.A. Kim, H.M. Gweon, Texture Analysis with 3.0-T MRI for Association of Response to Neoadjuvant Chemotherapy in Breast Cancer, Radiology 294 (2020) 31–41.

[24] D. Zhang, Q. Zhang, S. Suo, Z. Zhuang, L. Li, J. Lu, J. Hua, Apparent diffusion coefficient measurement in luminal breast cancer: will tumour shrinkage patterns affect its efficacy of evaluating the pathological response? Clin. Radiol. 73 (909) (2018) e907–909.e914.

[25] S.C. Partridge, Z. Zhang, D.C. Newitt, J.E. Gibbs, T.L. Chenevert, M.A. Rosen, P. J. Bolan, H.S. Marques, J. Romanoff, L. Cimino, B.N. Joe, H.R. Umphrey, H. Ojeda-Fournier, B. Dogan, K. Oh, H. Abe, J.S. Drukteinis, L.J. Esserman, N.M. Hylton, Diffusion-weighted MRI Findings Predict Pathologic Response in Neoadjuvant Treatment of Breast Cancer: The ACRIN 6698 Multicenter Trial, Radiology 289 (2018) 618–627.

[26] M. Iima, M. Honda, E.E. Sigmund, A. Ohno Kishimoto, M. Kataoka, K. Togashi, Diffusion MRI of the breast: Current status and future directions, J. Magn. Reson. Imaging 52 (1) (2020) 70–90.
[27] S.Y. Hahn, E.Y. Ko, B.K. Han, J.H. Shin, E.S. Ko, Role of diffusion-weighted imaging as an adjunct to contrast-enhanced breast MRI in evaluating residual breast cancer following neoadjuvant chemotherapy, Eur. J. Radiol. 83 (2014) 283–288.
[28] L. Minarikova, W. Bogner, K. Pinker, L. Valkovic, O. Zaric, Z. Bago-Horvath, R. Bartsch, T.H. Helbich, S. Trattnig, S. Gruber, Investigating the prediction value of multiparametric magnetic resonance imaging at 3 T in response to neoadjuvant chemotherapy in breast cancer, Eur. Radiol. 27 (2017) 1901–1911.
[29] H. Fujimoto, T. Kazama, T. Nagashima, M. Sakakibara, T.H. Suzuki, Y. Okubo, N. Shiina, K. Fujisaki, S. Ota, M. Miyazaki, Diffusion-weighted imaging reflects pathological therapeutic response and relapse in breast cancer, Breast Cancer 21 (2014) 724–731.
[30] P. Baltzer, R.M. Mann, M. Iima, E.E. Sigmund, P. Clauser, F.J. Gilbert, L. Martincich, S.C. Partridge, A. Patterson, K. Pinker, F. Thibault, J. Camps-Herrero, D. Le Bihan, Diffusion-weighted imaging of the breast-a consensus and mission statement from the EUSOBI International Breast Diffusion-Weighted Imaging working group, Eur. Radiol. 30 (2020) 1436–1450.
[31] E.A. Eisenhauer, P. Therasse, J. Bogaerts, L.H. Schwartz, D. Sargent, R. Ford, J. Dancey, S. Arbuck, S. Gwyther, M. Mooney, L. Rubinstein, L. Shankar, L. Dodd, R. Kaplan, D. Lacombe, J. Verweij, New response evaluation criteria in solid tumours: revised RECIST guideline (version 1.1), Eur. J. Cancer 45 (2009) 228–247.
[32] N.M. Hylton, J.D. Blume, W.K. Bernreuter, E.D. Pisano, M.A. Rosen, E.A. Morris, P. T. Weatherall, C.D. Lehman, G.M. Newstead, S. Polin, H.S. Marques, L.J. Esserman, M.D. Schnall, A.T. Team, I.S.T. Investigators, Locally advanced breast cancer: MR imaging for prediction of response to neoadjuvant chemotherapy–results from ACRIN 6657/I-SPY TRIAL, Radiology 263 (2012) 663–672.
[33] A. Ashraf, B. Gaonkar, C. Mies, A. DeMichele, M. Rosen, C. Davatzikos, D. Kontos, Breast DCE-MRI Kinetic Heterogeneity Tumor Markers: Preliminary Associations With Neoadjuvant Chemotherapy Response, Transl. Oncol. 8 (2015) 154–162.
[34] N.M. Hylton, C.A. Gatsonis, M.A. Rosen, C.D. Lehman, D.C. Newitt, S.C. Partridge, W.K. Bernreuter, E.D. Pisano, E.A. Morris, P.T. Weatherall, S.M. Polin, G. M. Newstead, H.S. Marques, L.J. Esserman, M.D. Schnall, A.T. Team, I.S.T. Investigators, Neoadjuvant Chemotherapy for Breast Cancer: Functional Tumor Volume by MR Imaging Predicts Recurrence-free Survival-Results from the ACRIN 6657/CALGB 150007 I-SPY 1 TRIAL, Radiology 279 (2016) 44–55.
[35] E. Bufi, P. Belli, M. Di Matteo, D. Terribile, G. Franceschini, L. Nardone, G. Petrone, L. Bonomo, Effect of breast cancer phenotype on diagnostic performance of MRI in the prediction to response to neoadjuvant treatment, Eur. J. Radiol. 83 (2014) 1631–1638.